Materials Today Advances 20 (2023) 100432

Contents lists available at ScienceDirect

Materials Today Advances

journal homepage: www.journals.elsevier.com/materials-today-advances/

Versatile, elastomeric and degradable polyHIPEs of poly(glycerol sebacate)-methacrylate and their application in vascular graft tissue-engineering

Samand Pashneh-Tala [a], Jonathan Field [a,b], Blanca Fornesa [c], Maite Molins Colomer [c], Caitlin E. Jackson [a,b], Mercedes Balcells [c,d], Jordi Martorell [c], Frederik Claeyssens [a,b,*]

[a] Department of Materials Science and Engineering, Kroto Research Institute, University of Sheffield, Sheffield, United Kingdom
[b] Department of Materials Science and Engineering, INSIGNEO Institute for in Silico Medicine, University of Sheffield, Sheffield, United Kingdom
[c] IQS School of Engineering, Universitat Ramon Llull, Barcelona, Spain
[d] Institute for Medical Engineering and Science, Massachusetts Institute of Technology, Cambridge, MA, United States

ARTICLE INFO

Keywords:
PolyHIPE
Poly(glycerol sebacate)
Porous polymers
Emulsion templating
Vascular graft
Tissue engineering

ABSTRACT

Polymer scaffolds are an important enabling technology in tissue engineering. A wide range of manufacturing techniques have been developed to produce these scaffolds, including porogen leaching, phase separation, gas foaming, electrospinning and 3D printing. However, all of these techniques have limitations. Delivering suitable scaffold porosity, small feature sizes and macroscopic geometry remain challenging.

Here, we present the development of a highly versatile scaffold fabrication method utilising emulsion templating to produce polymerised high internal phase emulsions (polyHIPEs) of the polymer poly(glycerol sebacate) methacrylate (PGS-M). PGS-M is biocompatible, degradable and highly elastic, with tunable mechanical properties. PGS-M was formulated into an emulsion using solvents and surfactants and then photocured into polyHIPE structures. The porosity, degradation behaviour, mechanical properties and biocompatibility of the PGS-M polyHIPEs was investigated.

The versatility of the PGS-M polyHIPEs was demonstrated with the production of various complex tubular scaffold shapes, using injection moulding. These shapes were designed for applications in vascular graft tissue engineering and included straight tubes, bends, branches, functioning valves, and a representative aortic arch. The PGS-M polyHIPE scaffolds supported vascular smooth muscle cells (SMCs) in 3D cell culture in a bioreactor.

1. Introduction

Scaffolds have been a foundation technology in the field of tissue engineering since its inception. These structures provide mechanical support and physical guidance to attached cells as they proliferate and form three-dimensional tissues [1–4]. A range of different materials have been used to produce tissue engineering scaffolds, with synthetic polymers being one of the most widely explored. These polymers offer increased versatility in terms of physical properties and processing routes compared to natural polymers. Scaffolds produced from synthetic polymers must be (i) biocompatible, to support healthy tissue growth; (ii) porous, to provide a large surface area for cell attachment and permit cell infiltration, mass transport and nutrient exchange; and (iii) degradable, so that they may be completely replaced by tissue over time [1–4].

Many different techniques have been developed for processing synthetic polymers into porous scaffolds suitable for tissue engineering. These include porogen leaching, phase separation, gas foaming, electrospinning and 3D printing [2–4]. These techniques all suffer from different limitations associated with their total porosity, the interconnectivity of their pores, or the shapes of the scaffolds that can be produced. For example, porogen leaching and gas foaming can produce structures with high porosity (>85 %), but pore interconnectivity is often limited [2,5]. Electrospinning produces porous, fibrous, scaffolds with high interconnectivity, however, the macroscopic geometry of the scaffolds is limited to flat, gently curved, or rolled sheets [6]. 3D printing methods can produce complex 3D scaffold designs with pore interconnectivity up to 100 %. However, resolution limitations prevent the

* Corresponding author. Department of Materials Science and Engineering, Kroto Research Institute, University of Sheffield, Sheffield, United Kingdom.
E-mail address: f.claeyssens@sheffield.ac.uk (F. Claeyssens).

https://doi.org/10.1016/j.mtadv.2023.100432
Received 20 July 2023; Received in revised form 23 September 2023; Accepted 7 October 2023
Available online 14 October 2023

inclusion of scaffold features on the length scales most suitable for tissue engineering (10s of μm) [1,7]. A need exists for a scaffold manufacturing system that can deliver high, interconnected, porosity and a variety of different complex shapes, representative of natural tissue structures.

Emulsion templating has emerged as a powerful technique for producing tissue engineering scaffolds using synthetic polymers [8–10]. In this method, an emulsion is formed from two immiscible phases; an internal phase, often a solvent such as water, dispersed as droplets in a polymer external phase. Polymerisation and solidification of the external phase and subsequent removal of the internal phase yields a porous structure. Pores are formed by the voids left after the removal of the internal phase droplets. Interconnectivity between pores is produced by the contact points between the internal phase droplets. Pore volume, size and interconnectivity can all be tuned by changing the emulsion formulation and processing parameters. This includes varying the ratio of the phases, adding viscosity modifiers, using surfactants, and altering the temperature or shear stress during mixing of the phases [8]. Emulsion templating enables highly porous and highly interconnected structures to be produced.

In general, emulsions with an internal phase >74.048 % (v/v) are considered high internal phase emulsions (HIPEs). This threshold value is based on the theoretical maximum packing density of uniform spherical droplets (monodisperse) in a finite volume as defined in the Kepler conjecture [11]. Although there exists some debate over this definition, due to the potential for variation in internal phase droplet size and deformation of the droplets, we will use this established convention here [8,12–15]. Subsequently, HIPEs that have been processed into porous structures by the polymerisation and solidification of their external phase and removal of their internal phase are termed polymerised high internal phase emulsions (polyHIPEs). A comprehensive review of polyHIPEs and their applications in tissue engineering can be found in the recent literature [8].

In addition to producing structures with highly interconnected pores, emulsion templating is also compatible with a wide range of processing methods suitable for liquids. The free-flowing emulsion may be cast, injection moulded, or 3D printed using stereolithography or extrusion based techniques [12,16–29]. These methods permit a variety of scaffold designs to be realised.

Despite the advantages offered by emulsion templating, in terms of porosity and the ability to produce constructs in many different shapes, this method of producing tissue engineering scaffolds has seen limited exploration. Emulsion templating is often completely overlooked when describing the suite of techniques used in tissue engineering scaffold manufacturing [2,3,30]. Of the work that has been reported, emulsion templating of elastomeric polymers yielding polyHIPE scaffolds suitable for soft tissue engineering is distinctly lacking.

Here, we report the use of the elastomeric polymer poly(glycerol sebacate) methacrylate (PGS-M) to produce polyHIPE tissue engineering scaffolds using emulsion templating. PGS-M is highly elastic with tunable mechanical properties in the kPa to MPa range for Young's modulus, making the material suitable for soft tissue applications [31,32]. PGS-M is also degradable and biocompatible [32]. We describe the synthesis and characterisation of PGS-M polyHIPEs, including porosity, degradation behaviour, mechanical properties and biocompatibility. The versatility of emulsion templating using PGS-M was demonstrated with the production of various complex tubular scaffold shapes suitable for applications in vascular graft tissue engineering. These scaffolds were created using injection moulding of PGS-M emulsions in directly and indirectly 3D printed moulds. Scaffold designs included straight tubes, bends, branches and functioning valves. Additionally, a representative aortic arch scaffold was produced to demonstrate the possibility of delivering patient-matched designs. The PGS-M polyHIPE scaffolds were also shown to support vascular smooth muscle cells (SMCs) in 3D cell culture.

2. Materials and methods

In the following methods, all chemical reagents were obtained from Merck, UK and all bioreactor components were obtained from Cole Parmer, UK, unless otherwise stated.

2.1. Synthesis of PGS-M prepolymer

PGS-M prepolymer was synthesised using methods described previously [32,33]. Briefly, PGS prepolymer was formed via the melt-polycondensation reaction of equimolar amounts of sebacic acid and glycerol (Fisher Scientific, UK). These were combined at 120 °C, under nitrogen gas for 24 h, followed by the application of a vacuum for a further 24 h.

The secondary hydroxyl groups of the glycerol subunits within the PGS prepolymer were then functionalised with methacrylate groups to produce the photocurable PGS-M prepolymer. 3.9 mmol of hydroxyl groups per gram of PGS prepolymer were available for methacrylation, based on both of the primary hydroxyl groups present in the glycerol having reacted with sebacic acid. The PGS prepolymer was dissolved 1:4 (w/v) in dichloromethane (Fisher Scientific, UK). Equimolar quantities of methacrylic anhydride and trimethylamine were then slowly added. Two different concentrations of methacrylic anhydride were used in order to generate PGS-M prepolymers with different degrees of methacrylation (DM). These were 0.5 and 0.8 mol/mol of PGS prepolymer hydroxyl groups, with the resulting PGS-M prepolymers further denoted as Low DM and High DM, respectively. 4-Methoxyphenol was also added at 1 mg/g of PGS prepolymer as a cross-linking inhibitor. The reaction was performed at 0 °C and allowed to rise to room temperature over 24 h. The solution was then washed with 30 mM hydrochloric acid (Fisher scientific, UK) at 1:1 (v/v) and dried with calcium chloride (Fisher scientific, UK). Finally, the dichloromethane was removed via rotary evaporation, under vacuum. Prepolymer characterisation is presented in the Supplementary material, Figure S1.

2.2. PGS-M HIPE synthesis

PGS-M polyHIPE scaffolds were formed from an emulsion. The emulsion consisted of an external phase, composed of PGS-M prepolymer combined with solvents, and an internal phase, composed of water. The two phases were stabilised using a surfactant.

Various combinations of polymer, solvent, water, surfactant and mixing speed were explored in order to produce a stable emulsion with a suitable porous structure once photocured. These are described in the Supplementary material (Table S1). The final emulsion composition is detailed below and was used to produce the polyHIPE scaffold structures throughout this study.

Dichloromethane and the surfactant Hypermer™ B246–SO-(MV) PSR0312/SAMP (kindly donated by Croda, UK) were mixed with PGS-M (Low DM or High DM) at ratios of 3:7 and 1:7 (w/w), respectively. Once the PGS-M and surfactant had fully dissolved, toluene was added at a ratio of 10:7 (toluene:PGS-M)(w/w) and the solution mixed at 200 rpm for 20 min using a stir bar. The PGS-M, dichloromethane, and toluene formed the external phase of the emulsion. To produce the emulsion, the mixing speed was increased to 300 rpm and dH_2O (internal phase) was slowly added. The ratio of the external phase to the internal phase (PGS-M, dichloromethane and toluene solution:dH_2O) was varied to explore the effect on the resulting polyHIPE structures. Ratios of 1:2, 1:3 or 1:4 (w/v) were examined. Once the emulsion had formed, the photoinitiator diphenyl(2,4,6-trimethylbenzoyl)phosphine oxide/2-hydroxy-2-methylpropiophenone (50/50 blend) (further denoted as photoinitiator) was added at 14:5 (PGS-M:photoinitiator)(w/w) and mixed in slowly by hand, using a fine, stainless steel, spatula. The emulsion was then aspirated into a syringe ready for dispensing and photocuring.

A typical volume of the emulsion was produced using 0.7 g PGS-M, 0.1 g surfactant, 0.3 g dichloromethane, 1 g toluene and 0.25 g of

photoinitiator, along with 4, 6 or 8 ml of dH_2O depending on the desired ratio of external phase to internal phase.

2.3. Fabrication of disc-shaped PGS-M polyHIPE scaffolds

Disc-shaped PGS-M polyHIPE scaffolds were manufactured for examination using various characterisation methods. To produce these scaffolds, an emulsion (HIPE) was prepared as described above and dispensed from a syringe into a two-part mould with a cylindrical cavity (40 mm × 8 mm diameter). The two-part mould was designed digitally (SolidWorks 2018, Dassault Systèmes, France) and 3D printed from a flexible and transparent material (Formlabs Form 2 with Elastic resin) (see Supplementary material, Figure S2). The emulsion was photocured inside the two-part mould using a UV LED array (Areacure, 365 nm, Integration Technology, UK). Two exposures of 15 s were used, with a 180° rotation in between. The resulting cylindrical polyHIPE structure was then removed from the mould and washed in methanol for 3 days, to remove any soluble prepolymer and residual photoinitiator, followed by dH_2O for a further 3 days. Methanol and dH_2O washed were refreshed daily. Finally, the PGS-M polyHIPE cylinder was cut into 1 mm thick discs using a razor blade.

2.4. Scanning electron microscopy of PGS-M polyHIPE scaffolds

Disc-shaped PGS-M polyHIPE scaffolds, produced as described above, were examined using scanning electron microscopy (SEM). PolyHIPE scaffolds were freeze-dried for 24 h, gold coated (Edwards S150B sputter coater) and then examined using SEM (FEI Inspect F50, Tescan Vega3 LMU) at 10–15 kV.

2.5. PGS-M polyHIPE scaffold porosity quantification using helium pycnometry

Disc-shaped PGS-M polyHIPE scaffolds were produced, as described above, and examined using helium pycnometry (AccuPyc 1340, Micromeritics, USA) to determine their porosity ($N = 2$, $n = 3$). 4 mm diameter discs were cut from wet scaffolds, using a dissection punch, and freeze-dried for 24 h. The diameters and thickness of the dry scaffolds were measured using digital callipers. These measurements were used to calculate the *macroscopic volume* of the scaffolds, ignoring their porosity. The scaffolds were then placed in the pycnometer, with a 0.1 cm^3 chamber insert installed, and the chamber pressurised with helium at 19,500 psi. The volume occupied by the scaffolds was then determined based on the volume of helium added. This was the *true volume* of the scaffolds, including their porosity. The scaffold porosity (%) was then calculated using Equation (1) [33]. Additionally, 4 mm diameter discs of commercially available Alvetex™ 3D cell culture scaffolds (Reprocell, UK) were also examined as positive controls.

$$\left(1 - \frac{true\ volume}{macroscopic\ volume}\right) \times 100 = Porosity\ (\%) \quad (1)$$

2.6. Degradation of PGS-M polyHIPE scaffolds in vitro

Degradation of the PGS-M polyHIPE scaffolds was examined using two treatments: cholesterol esterase enzyme (porcine pancreas) (40 units/ml) and PBS. Disc-shaped PGS-M polyHIPE scaffolds were produced using ratios of external to internal phase of 1:2, 1:3 and 1:4, as described above. The scaffolds were freeze-dried for 24 h and then weighed. The dry scaffolds were then placed in 1 ml of treatment solution and agitated on an orbital shaker, at 90 rpm, in an incubator at 37 °C and 5 % CO_2. Every 2 days the scaffolds were removed, dried to constant mass, reweighed and replaced in fresh treatment solution ($N = 2$, $n = 4$). Controls were untreated. Scaffolds were treated for a cumulative 6 days.

2.7. Tensile testing of PGS-M polyHIPE scaffolds

The mechanical properties of the PGS-M polyHIPE scaffolds were assessed by tensile testing (Mecmesin MultiTest 2.5-dV with 25 N load cell). As described above, emulsions were prepared from Low and High DM PGS-M, using ratios of external to internal phase of 1:2, 1:3 and 1:4. The emulsions were mixed with photoinitiator and aspirated into syringes. Injection moulding of the emulsion was used to produce tensile test pieces. The test piece design was based on the Type 3 dumb-bell, as specified in BS ISO 37:2011, with a 16 mm gauge length [34]. A custom, two-part, silicone elastomer (Sylgard™ 184, Dow, USA) mould was produced by casting in a digitally designed and 3D printed negative (Formlabs Form 2 with Grey resin). The silicone mould parts were held together between two transparent polystyrene plates, secured with stainless steel nuts, bolts and washers. The emulsions were injected into the silicone mould using 20G dispensing tips (Intertronics, UK) and then photocured, as described above. The resulting PGS-M polyHIPE tensile test pieces were then washed in methanol and dH_2O, as described above, and freeze-dried for 24 h. Tensile testing was performed at a crosshead speed of 500 mm/min with samples elongated to failure to determine effective Young's modulus (E_f), ultimate tensile strength (UTS) and strain at UTS ($N = 2$, $n = 4$).

2.8. Cell culture

Primary human vascular smooth muscle cells (SMCs) and immortalised mouse vascular smooth muscle cells were cultured on the PGS-M polyHIPE scaffolds. Human aortic SMCs were obtained commercially (PromoCell, Germany) and cultured to between passage 7 and 10 in specific growth medium (SMC growth medium 2 + supplement mixture, PromoCell, Germany). Mouse aortic SMCs immortalised by transfection with the SV40 large T antigen were obtained commercially (MOVAS, CRL-2797™, American Type Culture Collection, USA). These cells were also transduced with a gene for neomycin resistance. Mouse aortic SMCs were cultured in Dulbecco's modified Eagle's medium (DMEM) modified with 10 % (v/v) foetal calf serum and 0.2 mg/ml G-418 sulphate (Geneticin®, Thermo Fisher Scientific, USA), to maintain selection of the transformed cells. All cell cultures were incubated at 37 °C and 5 % CO_2.

2.9. In vitro cell metabolism and proliferation on PGS-M polyHIPE scaffolds

Disc-shaped PGS-M polyHIPE scaffolds were produced using a 1:4 ratio of external to internal phase, as described above. The scaffolds were sterilised using 3 washes with 70 % ethanol, followed by 3 washes with PBS, and then placed, individually, in the wells of a 96-well tissue culture plate.

Human aortic SMCs, cultured to between passage 7 and 10 as described above, were detached and resuspended in the appropriate growth medium at 1.925×10^6 cells/ml. 200 μl of the cell suspension was then seeded onto each polyHIPE scaffold (1×10^6 cells/cm^2 of scaffold surface seeded). The scaffolds were then placed in an incubator to allow the cells to attach. After 4 h, the growth medium was aspirated from the wells and the scaffolds were subsequently removed from the 96-well tissue culture plate and placed, individually, in the wells of a 12-well tissue culture plate. An additional 1 ml of growth medium was added to each culture well and the seeded scaffolds were returned to the incubator. The growth medium was refreshed every second day during culture. Equivalent, unseeded, PGS-M polyHIPE scaffolds were incubated in growth medium, in parallel, to act as negative controls.

At 24 h (1 day) and 7 days post-cell seeding, cell metabolism was assessed by reduction of resazurin sodium salt ($N = 2$, $n = 3$). 1 mM resazurin dissolved in dH_2O was filter sterilised, mixed 10 % (v/v) with the appropriate cell growth medium, and applied to each scaffold culture. After 4 h of incubation, 200 μl of the solution was extracted from

each well, in triplicate, placed in 96-well plates and examined using a fluorescence plate reader (Tecan Infinite® 200 Pro) at 540 nm excitation and 635 nm emission. The reading from a sample of incubated equivalent resazurin-containing growth medium acted as a blank.

In parallel with the examination of metabolic activity, additional cultured PGS-M polyHIPE scaffolds were also examined using histology. At the conclusion of the culture periods, the seeded scaffolds and unseeded controls were rinsed with three washes of PBS and then fixed with 3.7 % formaldehyde. The fixed scaffolds were then frozen in OCT compound (Tissue-Tek, Sakura, Japan) and cut into 5 μm sections at −25 °C (Lieca CM1860 UV), before being mounted on glass slides and stained with haematoxylin and eosin (H&E). Stained sections were imaged using light microscopy (Motic B5 professional series).

2.10. Chick chorioallantoic membrane (CAM) assay

The ex-vivo CAM assay was used to examine the potential toxic effects of the PGS-M polyHIPE scaffolds within a developing vascular system. Low and High DM PGS-M polyHIPE cylinders were produced from emulsions containing a 1:4 ratio of external to internal phase, as described above. Following washing, the polyHIPE cylinders were frozen at −20 °C for 4 h in preparation for sectioning. A vibratome (5100mz Campden Instruments, UK) was used to cut the polyHIPE cylinders into 200 μm thick discs. The frozen polyHIPE cylinders were positioned vertically in the vibratome reservoir. The reservoir was filled with cold water, covering the blade. Sections were cut using a frequency of 80 Hz, an amplitude of 1.50 mm and a speed of 0.10 mm/s. The resulting 200 μm thick polyHIPE discs were disinfected by submersion in methanol followed by 3 days in PBS (changed daily).

The CAM assay was conducted according to the methods described by Ramos-rodriquez et al. [35] Briefly, pathogen-free fertilised eggs (*Gallus Domesticus*) (Henry Stewart & Co., UK), were cleaned with a 20 % (v/v) solution of industrial methylated spirits and incubated in a humidified hatching incubator (Rcom King Suro Max-20, P&T Poultry, UK) at 38 °C. On embryonic development day (EDD) 3, the eggs were opened into sterile, 100 ml, weigh boats containing 3 ml of PBS solution with 1 % (v/v) penicillin (10,000 units/ml) and 1 % (v/v) streptomycin (10 mg/ml), and transferred to a cell culture incubator operating at 38 °C and 1 % CO_2. On EDD 7, the disinfected polyHIPE discs were implanted within the boundaries of the CAM and incubated for a further 5 days. On EDD 12, the CAM was imaged using a digital camera and MicroCapture software (version 2.0). Moisturising cream (Lacura, UK) was injected into the surrounding area of the sample to provide contrast between blood vessels and the sample. Following imaging, all embryos were sacrificed. All embryos were incubated and handled under the guidelines of the UK Home Office.

2.11. Scaffolds for vascular graft tissue engineering produced using emulsion templating

Tubular scaffolds suitable for applications in vascular graft tissue engineering were produced from PGS-M using emulsion templating. A HIPE was produced from Low DM PGS-M (1:4 ratio of external to internal phase). This was mixed with photoinitiator and loaded into a syringe, as described above. The HIPE was then injection moulded into flexible and transparent moulds to achieve the desired scaffold shapes. A variety of mould designs and configurations were used to produce straight, bent and bifurcated tubular scaffolds, along with scaffolds representing vein valves and the aortic arch (see Supplementary material). The PGS-M HIPE was photocured inside each mould using a UV LED array, as described above. The resulting polyHIPEs were then washed in organic solvents and dH_2O. (see Supplementary material for full details).

2.12. Cell seeding and "proof-of-concept" bioreactor culture of tissue-engineered vascular grafts using PGS-M polyHIPE scaffolds

Large diameter, straight, tubular PGS-M polyHIPE scaffolds and the aortic arch scaffolds were manufactured as described above and used as the basis for a "proof-of-concept" tissue engineered vascular graft. The PGS-M polyHIPE scaffolds were mounted in bespoke bioreactor systems. The bioreactors consisted of a digitally designed and 3D printed chamber (Formlabs Form 2 with Dental SG resin) with a polycarbonate lid and a simple flow circuit composed of flexible tubing (8 mm inner diameter, 11 mm outer diameter, C-Flex or Pharmed BPT) and nylon/polypropylene barbed and Luer Lock fittings (see Supplementary material, Figures S9 and S10). The flow circuits allowed fluid to move from the bioreactor chambers, through the scaffold lumens, and then back into the chambers, using a peristaltic pump (Masterflex L/S variable speed drive with Easy-Load PPS, SS rotor pump head). The chamber lids also featured two sterile 0.2 μm filters (Fisher Scientific, UK) fitted to silicone tubing lines. These filters permitted gaseous exchange and allowed growth medium to be added into the bioreactor chambers. Two large diameter, straight, tubular scaffolds were supported in a single bioreactor chamber, while only a single aortic arch scaffold was supported in its bioreactor chamber.

The assembled bioreactor systems, with mounted PGS-M polyHIPE scaffolds, were sterilised by autoclave. 50 ml of FCS was then added into the bioreactor chambers, via the sterile filter lines, and circulated through the flow circuit using the peristaltic pump. Once the FCS had filled the scaffolds, the flow was stopped and the scaffolds allowed to soak for 24 h. During this time, the bioreactor systems were moved into a cell culture incubator. The FCS was subsequently aspirated out of the bioreactor chambers and Mouse aortic SMCs (15×10^6 cells suspended in 8 ml of appropriate growth medium) seeded onto the lumen of each PGS-M scaffold. Working in a laminar flow cell culture cabinet, the flow circuits were opened immediately upstream of each scaffold, via a Luer Lock fitting, and the cell suspension delivered directly into the lumen of the scaffolds using a syringe. The flow circuits were then closed and clamped upstream and downstream of the scaffolds. To achieve even cell seeding across the scaffold lumens, the bioreactor systems were mounted on a custom rotating platform and rotated at 0.2 rpm for 4 h, inside a cell culture incubator. Following rotation, the clamps were removed from the flow circuits and 150 ml of appropriate growth medium added into the bioreactor chambers, via the sterile filter lines. The growth medium was circulated around the flow circuits and through the PGS-M scaffolds using the peristaltic pump at 6 rpm. Once the flow circuits were filled with growth medium, the pump was deactivated and the bioreactor systems placed in a cell culture incubator. After 24 h, the scaffolds were removed from the bioreactor chambers, rinsed with PBS and fixed with 3.7 % formaldehyde. The fixed scaffolds were then frozen, sectioned, stained with H&E, and imaged using light microscopy, as described above.

2.13. Statistical analysis

Data are displayed as mean ± standard deviation. Results were statistically analysed using GraphPad Prism software (version 9.0.2). Scaffold degradation and dimensional analysis (see Supplementary material, Figure S11) results were statistically analysed using one-way ANOVA with Tukey's multiple comparison analysis. Paired samples were specified in the assessment of the dimensional analysis data. Scaffold porosity, tensile testing, and metabolism assay results were statistically analysed using two-way ANOVA with Tukey's multiple comparison analysis. $P < 0.05$ was considered significant in all analyses.

3. Results

PGS prepolymer was functionalised with methacrylate groups producing PGS-M prepolymer. PGS prepolymer was synthesised by the

polycondensation reaction of glycerol with sebacic acid at 120 °C. GPC analysis determined the number average molecular weight (M_n) of the PGS prepolymer to be 1600 ± 234 g/mol and the weight average molecular weight (M_w) to be 5630 ± 1030 g/mol. Dispersity was 3.51 ± 0.17.

PGS-M prepolymer was produced with two different degrees of methacrylation (Low DM and High DM) by varying the molar ratio of methacrylic anhydride to PGS prepolymer OH groups used during synthesis. NMR analysis revealed the clear addition of the methacrylate groups in the functionalised prepolymer and spectral peaks were used to calculate the DM (See Supplementary material, Figure S1). The DM of the Low DM PGS-M was 41.4 % and 41.8 % for batches 1 and 2, respectively. The DM of the High DM PGS-M was 64.0 %.

PGS-M prepolymers were combined with organic solvents, water and a surfactant to produce a HIPE. Different combinations of prepolymer, solvents, water and surfactant were examined under different processing

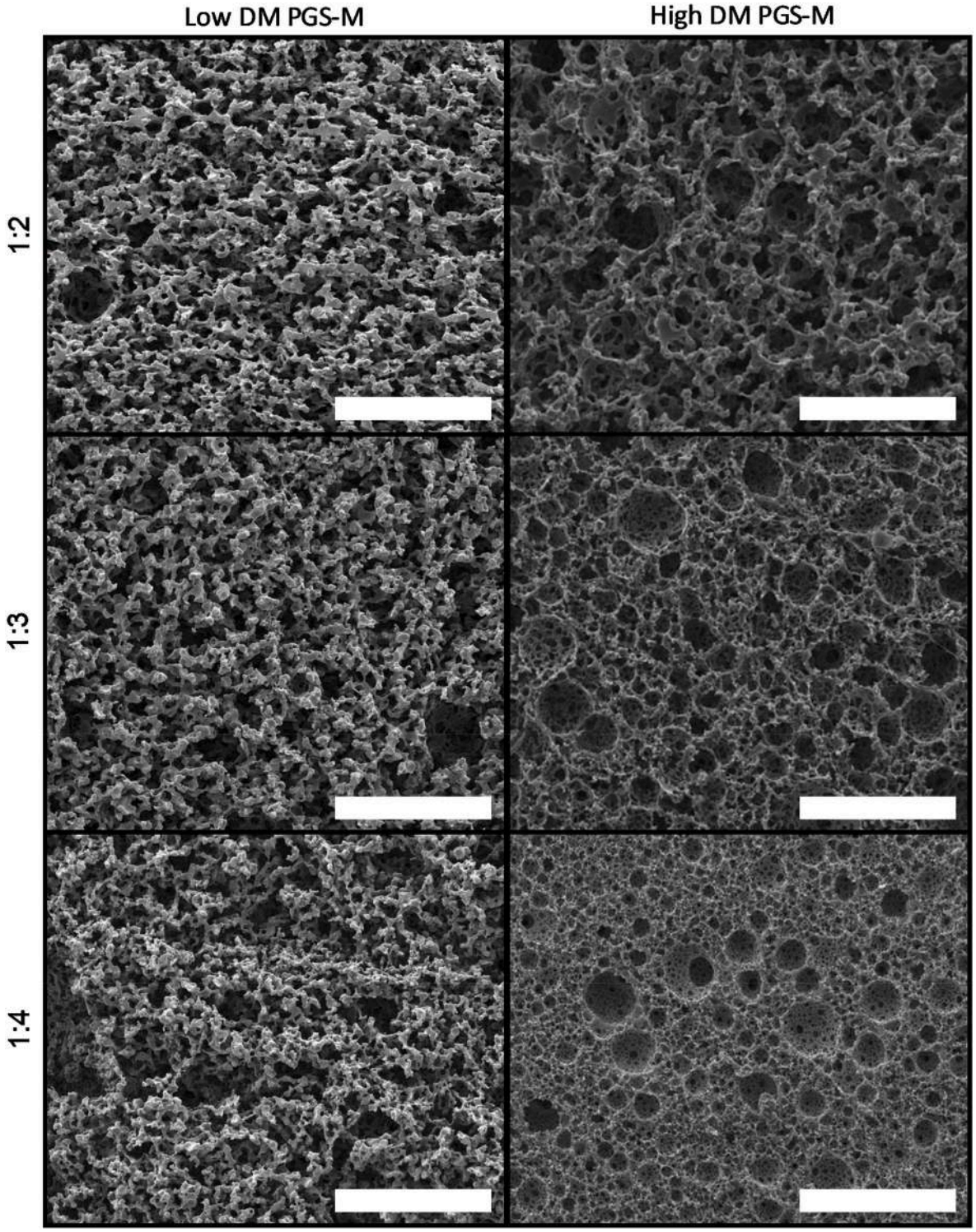

Fig. 1. SEM of Low and High DM PGS-M polyHIPE scaffolds produced using 1:2, 1:3 and 1:4 ratios of external to internal phase. All scaffolds appeared porous throughout their interiors. Scale bars are 200 μm.

conditions in order to produce a stable emulsion (see Supplementary material, Table S1). The most suitable emulsion composition was used to produce PGS-M polyHIPE scaffolds by photocuring, in combination with a photoinitiator.

The PGS-M polyHIPE scaffolds were examined using Raman spectroscopy. This confirmed the absence of residual photoinitiator following post-processing and washing (see Supplementary material, Figure S3).

Some shrinkage of the disc-shaped, PGS-M polyHIPE scaffolds was apparent compared to the original design dimensions. The mould used to produce the scaffolds had an inner diameter of 8 mm. However, after washing, the scaffolds produced using the Low and High DM PGS-M HIPE were 5.50 ± 0.23 mm and 6.40 ± 0.17 mm in diameter, respectively (see Supplementary material, Figure S11). There were no significant differences between the dimensions of PGS-M polyHIPE scaffolds produced using the same polymer, but different ratios of external to internal phase. The average shrinkage across the diameter of the scaffolds following photocuring and washing was therefore ~31 % and ~20 % for the Low and High DM PGS-M polyHIPE scaffolds, respectively. This difference in shrinkage was statistically significant. The scaffold dimensions were also further examined following freeze-drying, although there were no significant differences in diameter compared to their wet (washed) state in all cases.

SEM revealed the structure of the PGS-M polyHIPEs. Both the Low and High DM PGS-M polyHIPEs appeared porous throughout their interiors (Fig. 1). This was clear at all ratios of external to internal phase, from 1:2 to 1:4. Qualitatively, the High DM PGS-M scaffolds appeared different from the Low DM PGS-M scaffolds, with more strongly defined spherical pores/voids. Additionally, an increase in porosity could be observed in the High DM PGS-M scaffolds as the ratios of external to internal phase decreased. This was not evident in the Low DM PGS-M scaffolds. Pore sizes appeared to be on the order of 10s of microns, however, this was more difficult to estimate in the Low DM PGS-M scaffolds due to their far less well defined pores.

The porosity of the PGS-M polyHIPE scaffolds was quantified using helium pycnometry (Fig. 2). All scaffolds exhibited a porosity of >75 %. Scaffold porosity generally increased with decreasing ratios of external to internal phase in both Low and High DM PGS-M polymers. In the Low DM PGS-M scaffolds, ratios of 1:2 and 1:3 were not significantly different from each other, but ratio 1:4 was significantly different from both (see Supplementary material, Table S2). In the High DM PGS-M scaffolds, all ratios displayed significantly different porosity. Comparing across PGS-M polymer types, High DM PGS-M scaffolds were significantly more porous than Low DM PGS-M scaffolds at ratios of 1:3 and 1:4. There was no significant difference between the porosities of the scaffolds produced from Low and High DM PGS-M at ratio 1:2. All PGS-M scaffolds showed significantly lower porosity than the Alvetex™ control, which was over 90 % porous.

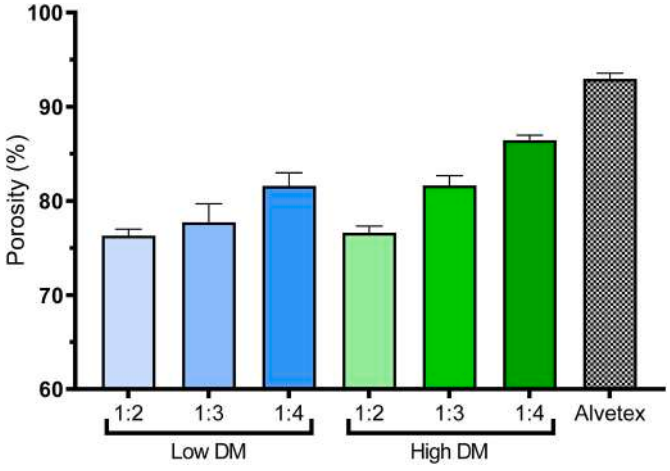

Fig. 2. Porosity of Low and High DM PGS-M polyHIPE scaffolds determined using helium pycnometry. Scaffolds were produced using HIPEs with ratios of external to internal phase of 1:2, 1:3 and 1:4. All scaffolds demonstrated porosities in excess of 75 %. Porosity was generally greater at decreased ratios of external to internal phase or at higher DM. The commercially available scaffold Alvetex™ acted as a positive control with a porosity exceeding 90 %.

PGS-M polyHIPE scaffold degradation was examined *in vitro* using cholesterol esterase enzyme to mimic the *in vivo* environment (Fig. 3). Degradation by hydrolysis alone was also examined using PBS. Significant degradation, measured as mass loss compared to dry control samples, was observed in almost all scaffold types as a result of the enzyme or PBS treatments. Only the High DM PGS-M polyHIPE scaffolds produced using a 1:4 ratio of external to internal phase showed no significant difference due to treatment with PBS after 6 days, compared to the control. Cholesterol esterase treatment produced greater degradation then PBS in all cases. Degradation was also greater in the Low DM PGS-M scaffolds compared to the High DM PGS-M scaffolds. The greatest degradation in the Low DM PGS-M scaffolds occurred at a ratio of external to internal phase of 1:3, with ~75 % mass remaining after 6 days of treatment with cholesterol esterase. The greatest degradation in the High DM PGS-M scaffolds also occurred at a ratio of external to internal phase of 1:3, with ~86 % mass remaining after 6 days treatment with cholesterol esterase.

The mechanical properties of the PGS-M polyHIPE scaffolds were determined using tensile loading. Low and High DM PGS-M polyHIPE scaffolds produced using ratios of external to internal phase of 1:2, 1:3 and 1:4 were tested to failure. Effective Young's modulus (E_f) was determined, along with ultimate tensile strength (UTS) and strain at UTS. The effective Young's modulus of the High DM PGS-M polyHIPE scaffolds was significantly greater than that of the Low DM PGS-M polyHIPE scaffolds in all cases (Fig. 4a, see Supplementary material, Tables S3 and S4 for statistical analysis results). Overall, effective Young's modulus reduced significantly with increasing internal phase content in both the Low and High DM PGS-M polyHIPEs. The Low DM polyHIPEs at ratios of external to internal phase of 1:2 and 1:3 were not significantly different, representing the exception. Theoretically predicted values for the effective Young's modulus of the PGS-M polyHIPEs were also calculated using Equation S2 in the Supplementary material. These predicted values overestimate effective Young's modulus in all cases; this was most pronounced in the Low DM PGS-M polyHIPEs. The trends seen in the effective Young's modulus values were also seen in the UTS values (Fig. 4b). The strain at which the UTS was reached appeared largely conserved across the different polyHIPE samples. Only the High DM polyHIPE at a ratio of external to internal phase of 1:3 was significantly different from any other sample (Fig. 4c, see Supplementary material, Table S5 for statistical analysis results).

Human aortic SMCs were seeded onto Low and High DM PGS-M polyHIPE scaffolds and cultured for up to 7 days. Reduction of the sodium salt resazurin demonstrated that cell metabolic activity was present on all scaffolds 1 day after seeding and there was no difference between cultures on the Low and High DM PGS-M scaffolds (Fig. 5a). Metabolic activity appeared to increase by 7 days post-seeding, although a statistically significant difference was only seen in the Low DM PGS-M scaffolds. Unseeded scaffold controls did not display any significant metabolic activity (see Supplementary material, Figure S12).

Histological examination of the seeded PGS-M polyHIPE scaffolds revealed cells at the scaffold's surfaces at 1 day post-seeding (Fig. 5b and c). There was evidence of migration into the porous interior of the scaffolds after 7 days, up to 400 μm in the High DM PGS-M scaffolds (Fig. 5d and e). Unseeded control scaffolds showed no evidence of cells (see Supplementary material, Figure S13).

PGS-M polyHIPE scaffolds were also implanted on the chorioallantoic membrane of developing chicks to assess their biocompatibility in a developing vascular system. Both Low and High DM PGS-M scaffolds appeared well tolerated by the developing embryo. There was no

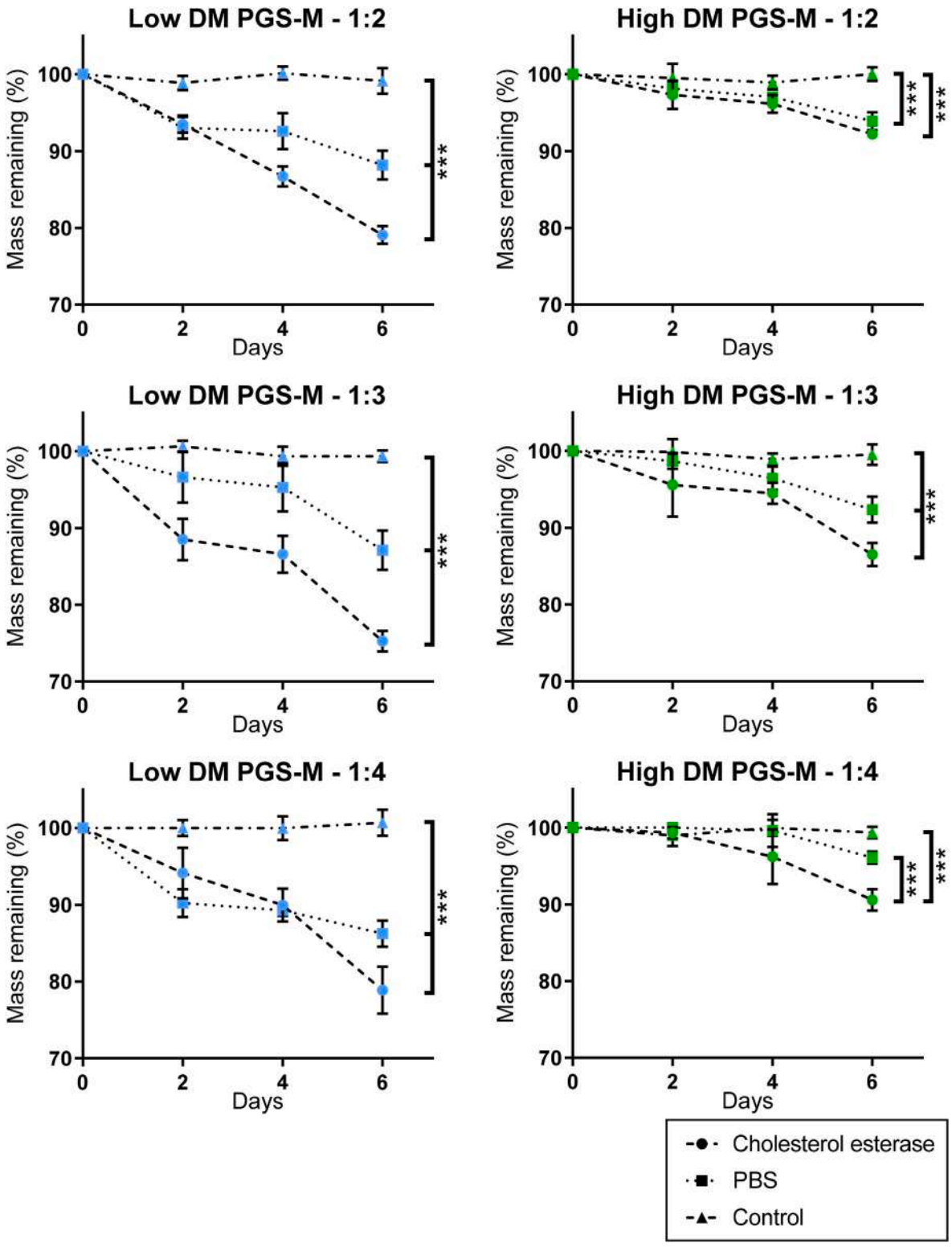

Fig. 3. Degradation of Low and High DM PGS-M polyHIPE scaffolds treated with cholesterol esterase and PBS. Scaffolds were produced using ratios of external to internal phase of 1:2, 1:3 and 1:4. Controls were untreated, dry scaffolds. Degradation was greatest in Low DM PGS-M scaffolds and as a result of enzymatic treatment.

evidence of toxicity around the scaffolds with clear uninterrupted development of the chick's vascular system proximal to the scaffolds (Fig. 5f and g).

Using injection moulding techniques, more complex polyHIPE scaffolds were produced from Low DM PGS-M. Tubular scaffolds for possible applications in vascular graft tissue engineering were demonstrated. These included simple straight tubes (Fig. 6a); bent, undulating, tubes (Fig. 6b); and branched tubes representing a uniform bifurcation and a theorised surgical anastomosis (Fig. 6c and d, respectively). These were all produced with an internal diameter of 3 mm. Additionally, a larger scaffold representing a vein valve, with an internal bileaflet arrangement, was also produced (Fig. 6e and f). All tubular PGS-M scaffolds

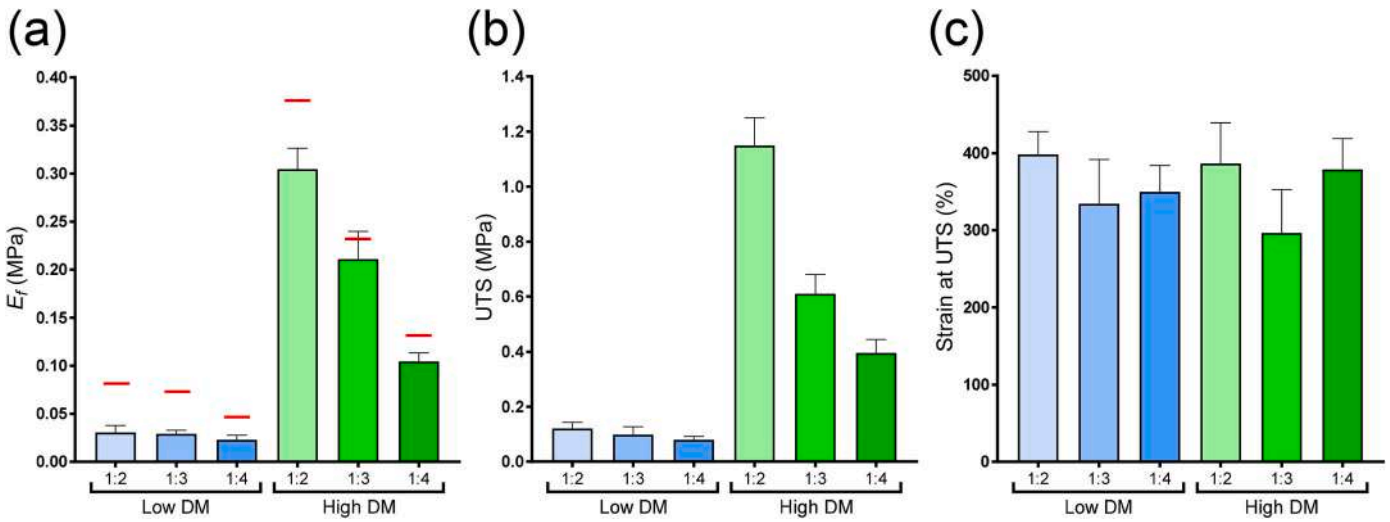

Fig. 4. Tensile testing of Low and High DM PGS-M polyHIPE scaffolds produced using ratios of external to internal phase of 1:2, 1:3 and 1:4. (a) Effective Young's modulus (E_f) of the polyHIPEs, Bars are experimentally determined results, red lines are theoretically predicted values. (b) Ultimate tensile strength (UTS) of the polyHIPEs. (c) Strain at UTS in the polyHIPEs. Greater values for effective Young's modulus and UTS were associated with the High DM PGS-M polymer or lower internal phase content. Strain at UTS is largely conserved across the different polyHIPEs.

were produced with high fidelity, with small features such as bifurcation branch points and valve leaflets well-defined.

As a proof-of-concept for vascular graft tissue engineering, large diameter, straight, tubular PGS-M polyHIPE scaffolds were mounted in a simple perfusion bioreactor system and seeded with mouse aortic SMCs. The PGS-M scaffolds had an outer diameter of 10 mm and an internal diameter of 8 mm (Fig. 7a). The scaffolds were assembled within the bioreactor system, sterilised, and then seeded with cells followed by rotation to achieve even cell coverage across their luminal surfaces. The seeded scaffolds were cultured for 24 h under static conditions and then fixed (Fig. 7b and c). Sections stained with H&E showed the clear presence of SMCs across the luminal surface of the tubular PGS-M scaffolds (Fig. 7d and Supplementary material, Figure S14). The cells also appeared to have penetrated into the porous scaffold up to 300 μm in some regions.

As a further demonstration of the value of our approach for producing scaffolds for vascular graft tissue engineering, a scaffold representative of the aortic arch of a human subject was also examined using bioreactor culture (Fig. 8). The PGS-M polyHIPE scaffold was designed based on human anatomy and then produced at 50 % scale compared to the native adult vessel size. The scaffold was mounted in another bespoke bioreactor system with a simple perfusion flow circuit. Mouse aortic SMCs were seeded onto the scaffold lumen and the bioreactor was again rotated to achieve even cell distribution (see Supplementary material, Figure S15). Following 24 h of static culture, the scaffold was removed, fixed and sectioned. Histology revealed that SMCs had lined the luminal surface of the scaffold. As seen in the large diameter, straight, tubular scaffolds, the cells grew into the porous scaffolds.

4. Discussion

Although a number of manufacturing methods for fabricating polymer tissue engineering scaffolds have been established, these are often constrained by various common limitations. Delivering suitable scaffold porosity, small feature sizes and macroscopic geometry remain challenging. Our results demonstrate that emulsion templating using PGS-M polyHIPEs is able to overcome many of these limitations making the approach highly versatile and attractive for scaffold fabrication.

PGS-M was synthesised and then successfully incorporated into a HIPE. Characterisation of the PGS-M material using GPC and NMR spectroscopy showed comparable results to those previously reported using the same or similar reaction conditions [32,36–41]. The PGS-M prepolymer was combined with organic solvents (DCM and toluene), a surfactant, and water to form a HIPE. Solvents were required to reduce the viscosity of the PGS-M prepolymer external phase sufficiently to permit sufficient mixing with the water internal phase [17,18,42]. There is a narrow operating range for the viscosity of the external phase in the formation of HIPEs - low enough to permit suitable mixing, but high enough to maintain stability and prevent emulsion breakdown [8,12,19]. This was clear in our initial studies to develop a suitable emulsion formulation. Best results were achieved using a combination of toluene with DCM. Mixtures of organic solvents have been shown to be beneficial in HIPE formation previously [12]. Herein, it is believed that beyond viscosity modification, the DCM also ensured dissolution of the waxy surfactant, enabling it to effectively mix into the emulsion and act as a stabilising agent.

SEM examination revealed the PGS-M polyHIPEs contained characteristic highly interconnected pores. This is a significant advantage of using emulsion templating to produce tissue engineering scaffolds compared to established methods such as porogen leaching and gas foaming which often have more limited pore interconnectivity [2,5]. The porosity of the polyHIPEs could be tuned, increasing as the ratio of external to internal phase decreased from 1:2–1:4 in both the Low and High DM PGS-M samples. The porosity of polyHIPEs is largely determined by the internal phase volume within the emulsion. However, the volume (%) of the internal phase does not necessarily translate directly into porosity (%) within the polyHIPE, due to solvent loss reducing the volume of the external phase [12,43]. Dimensional analysis of the PGS-M polyHIPEs showed that shrinkage of up to ~31 % occurred compared to the cast dimensions and this was more pronounced in the Low DM PGS-M polyHIPEs, likely due to their lower stiffness. Pore sizes appeared to be in the range if 10–100 μm, although these could only be reasonably estimated in the High DM PGS-M polyHIPEs, due to some structural collapse in the Low DM PGS-M samples resulting in a lack of well-defined, spherical, pores [17,28]. These pore sizes are comparable to those observed in other degradable polyHIPE scaffolds produced for tissue engineering applications [8,12,18,23,28,29,44].

Emulsion templating can therefore deliver PGS-M scaffolds with highly interconnected and tunable porosity, although the dimensions of the final scaffold design must be carefully considered due to the potential for scaffold shrinkage. In future work, the emulsion may be optimised further by fine-tuning the hydrophilic−lipophilic balance

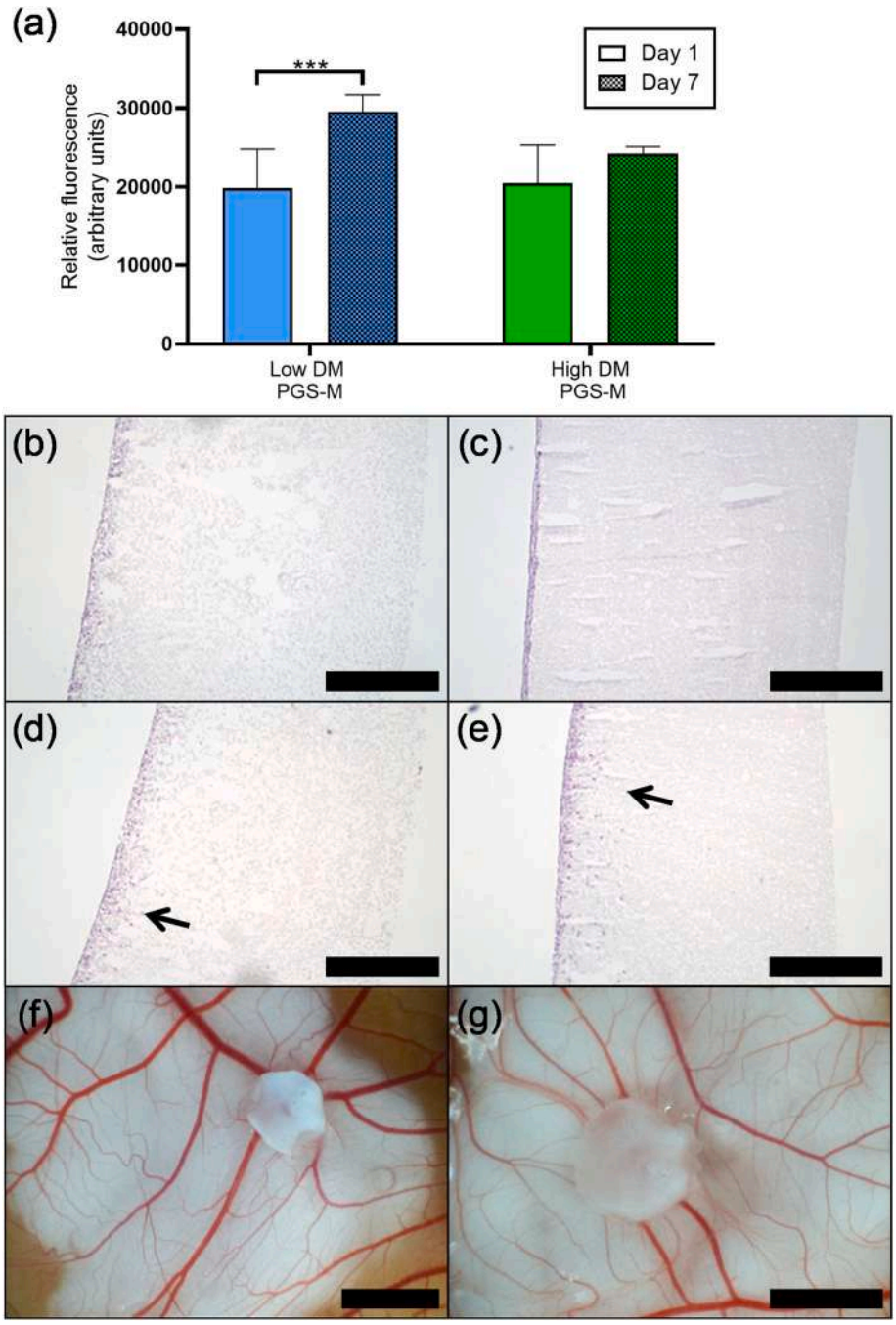

Fig. 5. Biocompatibility of PGS-M polyHIPE scaffolds. Low and High DM PGS-M scaffolds supported cell metabolism over 7 days of *in vitro* culture with human aortic SMCs (a). H&E staining showed seeded cells at the surface of both the Low and High DM PGS-M scaffolds ((b) and (c), respectively), and also penetrating deeper into the scaffolds' interiors after 7 days ((d) and (e), respectively). Arrows mark the maximum depth of cell penetration. The CAM assay demonstrated that both Low and High DM PGS-M polyHIPE scaffolds were tolerated by a developing vascular system with no visible toxic effects ((f) and (g), respectively). Scale bars are 500 μm in (b)–(e), and 5 mm in (f) and (g).

(HLB) value of the surfactant to vary pore size and interconnectivity while maintaining emulsion stability [8,17].

The degradation and mechanical behaviour of PGS-M scaffolds can be tuned by altering the DM of the polymer [32]. Increasing the DM reduces degradation rates and increases stiffness and strength. Emulsion templating enables further modulation of these properties by controlling the porosity of the scaffolds through the emulsion composition. Degradation of the PGS-M polyHIPE scaffolds was enhanced by increased porosity. Mass loss due to enzyme or PBS treatment over 6 days was greater in the polyHIPE scaffolds compared to similar bulk PGS-M samples examined previously (maximum of ~25 % vs ~3 %, respectively) [32]. This was likely due to the increased surface area of the polyHIPE scaffolds. Degradation of polyHIPE tissue engineering scaffolds has not been studied well, even though this affects extracellular matrix (ECM) deposition and tissue integrity significantly. Reports are limited to treatments in cell culture medium or NaOH solution which do not represent *in vivo* conditions [28,45,46]. To our knowledge, this is the first report of the degradation of a polyHIPE tissue engineering scaffold under conditions intended to mimic the *in vivo* enzymatic environment [47]. The results indicate a relatively rapid *in vivo* degradation by the PGS-M polyHIPE and this may be advantageous. In tissue-engineered blood vessels, rapid scaffold degradation has been linked to enhanced

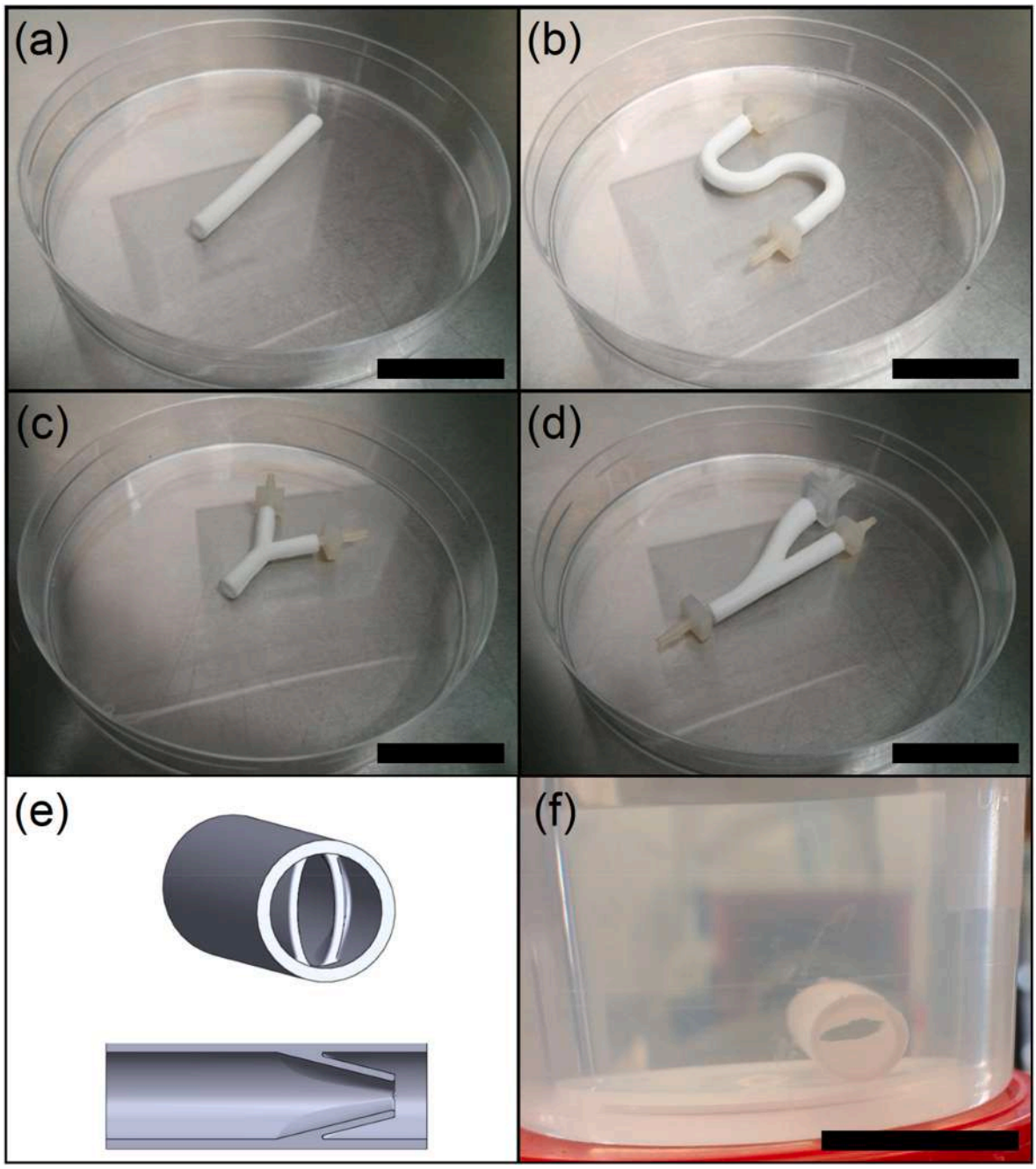

Fig. 6. Tubular PGS-M polyHIPE scaffolds for vascular graft tissue engineering produced using injection moulding. Various designs were produced with an internal diameter of 3 mm, including straight tubes (a); bent, undulating, tubes (b); uniform bifurcations (c); and a theorised surgical anastomosis (d). A larger diameter, vein valve scaffold was also designed (e) and produced. When suspended in PBS, the internal valve leaflets could be clearly seen (f). Scale bars are 20 mm.

ECM deposition and tissue remodelling [48,49].

Tensile testing showed that the mechanical properties of the PGS-M polyHIPE scaffolds varied based on their porosity and the DM of the polymer. Increased porosity resulted in lower values for effective Young's modulus and UTS, as a result of reduced material across the scaffold cross-section. Interestingly, the strain at which UTS was reached was largely conserved between the Low and High DM samples. This suggested that the stiffer High DM PGS-M is able to elongate to the same degree as the Low DM PGS-M while achieving a higher UTS. It has been shown that the effective Young's modulus of open cell foams, such as the PGS-M polyHIPEs, can be related to the Young's modulus of the bulk foam material [44]. Applying this relationship yielded theoretical values of effective Young's modulus for the PGS-M polyHIPEs which compared moderately well with the experimentally determined results. The theoretical values overestimate the effective Young's modulus in all cases. This may be due to the previously discussed deformation and partial collapse of the pores in the PGS-M scaffolds leading to an understatement of their macroscopic volume. The results do suggest that an estimate of the effective Young's modulus of PGS-M polyHIPEs can be made using only the sample porosity and bulk mechanical properties.

The effective Young's modulus values of the PGS-M polyHIPEs are generally lower than those reported for other degradable polyHIPEs. For example, methacrylate functionalised PCL polyHIPEs and thiol-ene/thiol-yne polyHIPEs displayed effective Young's modulus values of ~0.20–0.52 MPa [12,23,50]. Although direct comparisons are difficult to draw, our data suggest that the PGS-M polyHIPEs are some of the most

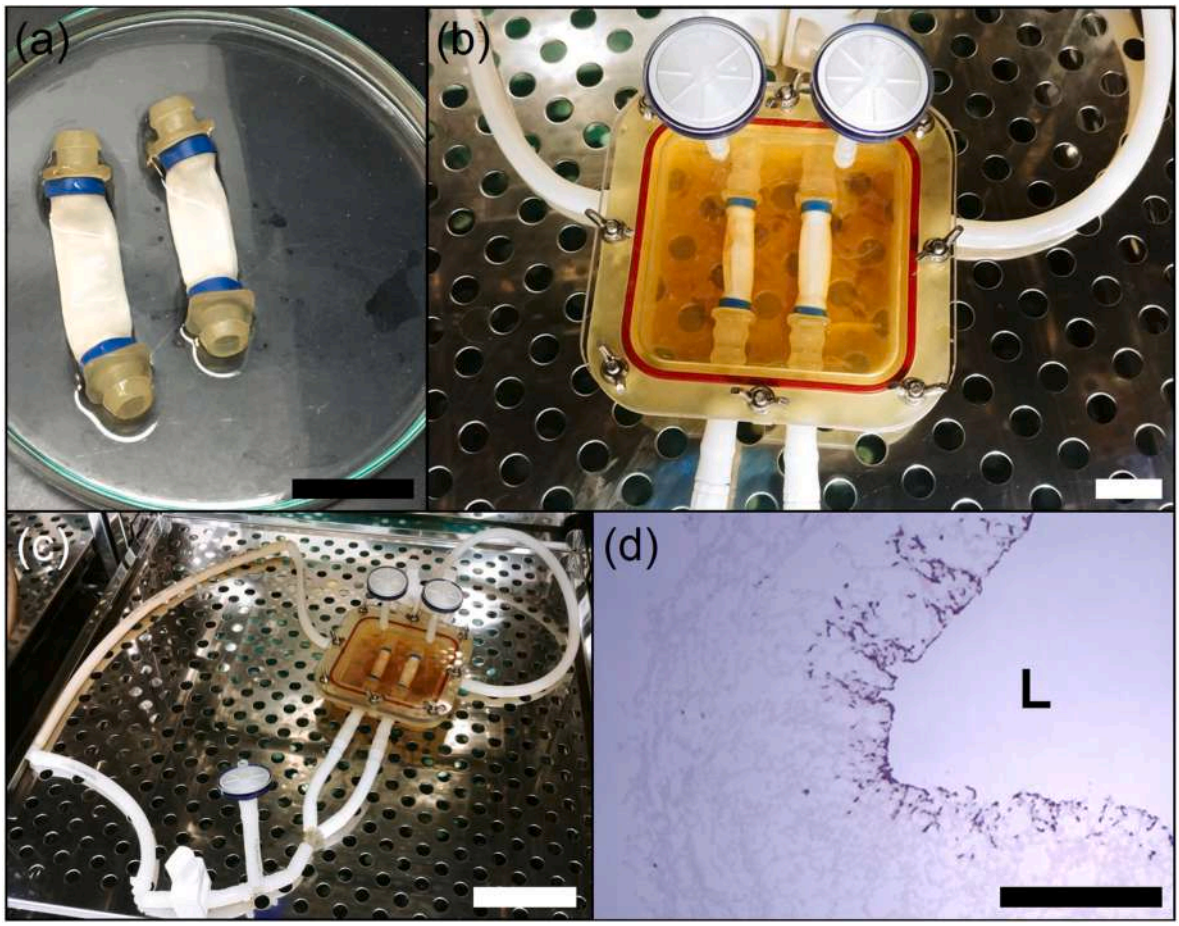

Fig. 7. Bioreactor culture of straight, tubular PGS-M polyHIPE scaffolds seeded with mouse aortic SMCs as proof-of-concept for vascular graft tissue engineering. (a) Large diameter, straight, tubular PGS-M polyHIPE scaffolds. (b) Scaffolds mounted inside bioreactor chamber. (c) Simple perfusion bioreactor system under static culture. (d) Seeded scaffold sections stained with H&E showing SMCs present on the luminal surface and penetrating into the scaffold interior. Luminal space denoted by "L". Scale bars are 20 mm in (a) and (b), 10 cm in (c) and 500 μm in (d).

elastomeric degradable polyHIPEs yet described. The PGS-M polyHIPEs may therefore be particularly useful in soft tissue applications. Of additional note is that the PGS-M polyHIPEs displayed comparable or higher UTS values compared with stiffer polyHIPEs [12]. This shows that PGS-M can produce both elastomeric and strong polyHIPEs compared to previously reported materials.

Both the Low and High DM PGS-M polyHIPE scaffolds supported the growth and proliferation of human aortic SMCs over 7 days. Although the metabolic activity of the cell cultures on both of the scaffold types appeared relatively equal 24 h after seeding, there was a significant difference after 7 days, with increased activity on the Low DM PGS-M scaffolds. This suggests that cell growth and proliferation may have been favoured in this environment, possibly due to the lower stiffness of the material better recreating the native environment of the cells. The SMCs proliferated and migrated into the interiors of both polyHIPE scaffold types. Similar results were observed in other polyHIPE scaffolds based on acrylate and methacrylate functionalised PCL [12,18,28,45,51]. This demonstrates an advantage of the highly interconnected porous structure of polyHIPEs, as this promotes cell infiltration.

Additionally, both the Low and High DM PGS-M polyHIPEs showed favourable results in the CAM assay. In both cases, the embryos developing vascular system was not disrupted by the presence of the polyHIPE scaffolds. This suggests the scaffolds were non-toxic, as this would have resulted in a clear boundary forming around them or, in the extreme, death of the developing embryo. These promising results indicate for the first time the potential of PGS-M scaffolds for use *in vivo*.

Both the cell culture and CAM assay results provide assurance that the use of emulsion templating does not potentially compromise scaffold biocompatibility, as a result of residual toxic agents used during scaffold preparation [32,33]. The solvents and surfactant were effectively washed out of the scaffolds in post-processing. Additionally, Raman spectroscopy confirmed the polymer composition of the scaffolds, as previously [33], and also the successful elimination of any residual PI. The spectral peaks associated with the PI, at 1000 and 3070 cm^{-1}, were substantially reduced after washing. The concentration of PI used in the formation of the PGS-M polyHIPEs was higher than that used in previous works on other degradable polyHIPEs, more than double in some cases [23,28,46]. This elevated concentration was required to achieve successful photocuring, possibly due to the PI being added after emulsion formation. It was therefore crucial to confirm suitable removal of any PI residue.

We demonstrated the use of casting and injection moulding to produce polyHIPE scaffolds from PGS-M. Casting is a common method for creating polyHIPE scaffolds, however, injection moulding has been largely unexploited. Herein, the use of directly and indirectly 3D printed moulds and soluble mould cores for injection moulding of polyHIPEs allowed a wide range of scaffold geometries to be realised.

PolyHIPE tissue engineering scaffolds with complex geometries have previously been produced using 3D printing techniques. Using emulsions enabled the minimum feature size limitations of the 3D printing systems to be overcome. Inherent porosity, on the μm scale, was delivered by the internal phase of the emulsions. Stereolithography and extrusion methods have been used to manufacture various polyHIPE scaffold designs, such as woodpiles and strut-based structures. However,

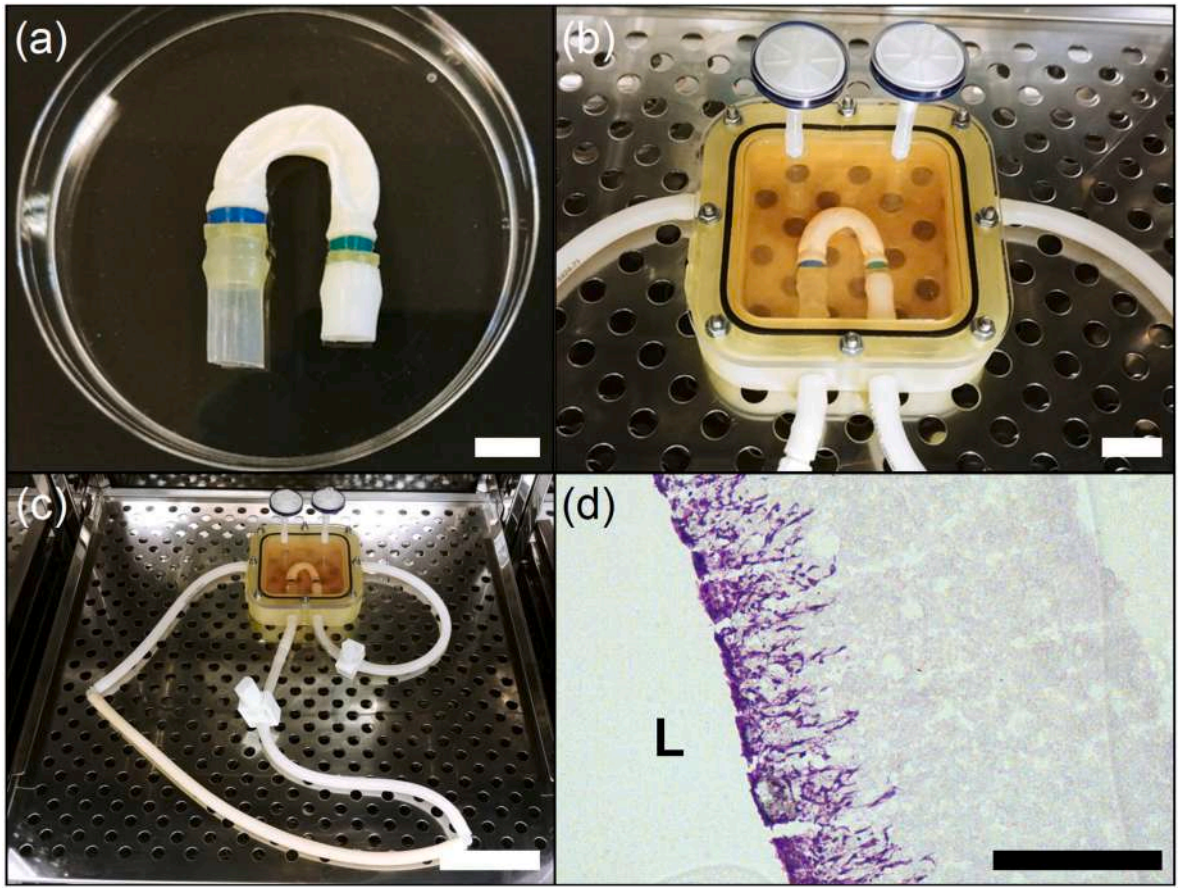

Fig. 8. Bioreactor culture of a PGS-M polyHIPE scaffold in the shape of the aortic arch. The scaffold was seeded with mouse aortic SMCs. (a) PGS-M polyHIPE scaffold representing the aortic arch. (b) Scaffold mounted inside bioreactor chamber. (c) Simple perfusion bioreactor system under static culture. (d) Seeded scaffold sections stained with H&E. SMCs were present on the luminal surface of the scaffold and penetrated into its interior. Luminal space denoted by "L". Scale bars are 10 mm in (a), 20 mm in (b), 10 cm in (c) and 400 μm in (d).

these scaffold designs have been limited by long manufacturing times and the requirement for supporting structures to permit overhanging features [16,21,22,24–27,29,52]. Alternatively, different combinations of other established manufacturing methods have been proposed to deliver complex porous scaffold geometries. Electrospun mats in combination with gas foaming in moulds has been explored [53,54], as has injection moulding of degradable polymers with NaCl porogens [55]. In both cases, however, only simple shapes have been demonstrated so far. In our previous work, we combined porogen leaching with both additive and subtractive manufacturing methods to enable the production of porous PGS-M scaffolds in a wide range of mm-cm scale geometries [33]. Although effective, these hybrid manufacturing strategies required bespoke or expensive equipment to be implemented. Emulsion templating of polyHIPEs using injection moulding allows a wide variety of porous scaffold geometries to be delivered, overcoming many of the limitations of previous scaffold fabrication methods. The use of desktop 3D printing in the workflow also reduces costs and increases accessibility.

We showed the potential of our PGS-M polyHIPE fabrication technology by producing scaffolds suitable for vascular graft tissue engineering. This is an area of great clinical need and the geometry of the natural vascular tree represents an excellent demonstration case for any novel tissue engineering scaffold manufacturing process [56,57]. Our method delivered an almost complete range of natural blood vessel shapes; including straight and curved tubes; bifurcations; and even bileaflet valves. The use of a soluble mould core, made from polycarbonate, also allowed the production of a scaffold representative of the aortic arch, with its 180° curvature. Of note is that the process to design this scaffold could easily be adapted to use medical scan data obtained from a human subject. Therefore, the potential exists for truly bespoke, patient-matched, vascular grafts to be designed, enabling personalised medical therapies. We showed that our polyHIPE vascular graft scaffolds could be cellularised with SMCs whilst positioned inside perfusion bioreactor systems. Similar results were observed in the large diameter, straight, tubular scaffold and the aortic arch scaffold suggesting no adverse effects associated with using the soluble mould core during scaffold manufacturing. Extended culture under pulsatile flow is now required to further develop this technology. Cells were able to proliferate and migrate up to 300 μm into the polyHIPE scaffold interiors over just 24 h. This is superior to the results reported when using porous PGS polymer scaffolds produced by porogen leaching, demonstrating an advantage provided by the interconnectivity of polyHIPE scaffolds [58].

Few efforts to generate tissue-engineered vascular grafts with complex geometries have been reported. Some success has been shown *in vivo* using electrospun scaffolds, however, the shapes produced were still relatively simple [59,60]. Alternatively, methods employing direct scaffold 3D printing or bioprinting are hampered by printing resolution, fabrication time and materials [61–71].

PGS-M is an ideal scaffold material for tissue-engineered vascular grafts due to its elasticity, degradability and biocompatibility [32,57]. This, coupled to the versatility of emulsion templating represents a promising starting point for vascular graft tissue engineering. Added to this, the ability to tune the mechanical properties of PGS-M further extends the utility of the polyHIPE scaffolds to other soft and hard tissue engineering applications requiring complex shapes.

5. Conclusion

We have capitalised on the favourable properties of PGS-M to enable the flexible production of highly porous polyHIPE tissue engineering scaffolds via emulsion templating. Our work has shown that polyHIPE porosity and mechanical properties can both be controlled through emulsion processing and that PGS-M produces some of the most elastomeric, degradable, polyHIPEs reported so far.

We have further demonstrated the versatility of our approach by fabricating many diverse polyHIPE scaffold geometries using injection moulding, enabled by 3D printing. Our PGS-M polyHIPE technology offers the flexibility to deliver macro-scale, anatomically relevant, scaffold geometries with inherent, highly interconnected, micro-scale porosity. We have therefore established PGS-M polyHIPEs as a valuable platform technology for tissue engineering.

Author contributions

Samand Pashneh-Tala: Conceptualisation, Investigation, Methodology, Supervision, Validation, Funding acquisition, Writing – original draft. Jonathan Field: Investigation, Methodology, Writing – review & editing. Blanca Fornesa: Investigation, Methodology, Writing – review & editing. Maite Molins Colomer: Investigation, Methodology, Writing – review & editing. Caitlin Jackson: Investigation, Methodology, Writing – review & editing. Mercedes Balcells: Methodology, Validation, Funding acquisition, Supervision, Writing – review & editing. Jordi Martorell: Methodology, Validation, Funding acquisition, Supervision, Writing – review & editing. Frederik Claeyssens: Conceptualisation, Investigation, Methodology, Validation, Funding acquisition, Supervision, Writing – review & editing.

Declaration of competing interest

The authors declare that they have no known competing financial interests or personal relationships that could have appeared to influence the work reported in this paper.

Data availability

Data will be made available on request.

Acknowledgements

The author(s) disclosed receipt of the following financial support for the research, authorship, and/or publication of this article: SPT and FC thank the Engineering and Physical Sciences Research Council (EPSRC) for a Doctoral prize fellowship (EP/M506618/1) and Impact Acceleration Account (EP/×525790/1), and the Medical Research Council for a Confidence in Concept award (MR/L012669/1). CEJ and FC thank the EPSRC, centre for doctoral training in Advanced Biomedical Materials PhD studentship funding (EP/S022201/1). FC also thanks the Royal Society for the funding of a Royal Society Leverhulme Trust Senior Research Fellowship 2022 (SRF\R1\221053). MB thanks Fundacio Empreses Institut Quimic de Sarria, La Caixa Foundation (Health Research 2019–198898), MISTI Global Seed Fund, the Ministerio de Ciencia e Innovacion (PID2021-124868OB-C21 and CPP2021-008438). JM the thanks the Ministerio de Ciencia e Innovacion (PID2021-124868OB-C21 and CPP2021-008438). We also thank Niall Paterson, Vincent Nelis and Robbie Brodie from Vascutek Ltd. (Terumo Aortic (UK)) for advise and financial support.

Appendix A. Supplementary data

Supplementary data to this article can be found online at https://doi.org/10.1016/j.mtadv.2023.100432.

References

[1] F. Zhang, M.W. King, Biodegradable polymers as the pivotal player in the design of tissue engineering scaffolds, Adv. Healthcare Mater. 9 (2020), 1901358.
[2] A. Eltom, G. Zhong, A. Muhammad, Scaffold techniques and designs in tissue engineering functions and purposes: a review, Adv. Mater. Sci. Eng. 2019 (2019), e3429527.
[3] P. Zhao, et al., Fabrication of scaffolds in tissue engineering: a review, Front. Mech. Eng. 13 (2018) 107–119.
[4] V. Raeisdasteh Hokmabad, S. Davaran, A. Ramazani, R. Salehi, Design and fabrication of porous biodegradable scaffolds: a strategy for tissue engineering, J. Biomater. Sci. Polym. Ed. 28 (2017) 1797–1825.
[5] X. Liao, H. Zhang, T. He, Preparation of porous biodegradable polymer and its nanocomposites by supercritical CO2 foaming for tissue engineering, J. Nanomater. 2012 (2012), e836394.
[6] T. Lu, Y. Li, T. Chen, Techniques for fabrication and construction of three-dimensional scaffolds for tissue engineering, Int. J. Nanomed. 8 (2013) 337–350.
[7] P. Bajaj, R.M. Schweller, A. Khademhosseini, J.L. West, R. Bashir, 3D biofabrication strategies for tissue engineering and regenerative medicine, Annu. Rev. Biomed. Eng. 16 (2014) 247–276.
[8] B. Aldemir Dikici, F. Claeyssens, Basic principles of emulsion templating and its use as an emerging manufacturing method of tissue engineering scaffolds, Front. Bioeng. Biotechnol. 8 (2020).
[9] T. Zhang, R.A. Sanguramath, S. Israel, M.S. Silverstein, Emulsion templating: porous polymers and beyond, Macromolecules 52 (2019) 5445–5479.
[10] M.S. Silverstein, Emulsion-templated polymers: contemporary contemplations, Polymer 126 (2017) 261–282.
[11] T. Hales, et al., A formal proof of the kepler conjecture, Forum Math. Pi 5 (2017).
[12] B. Aldemir Dikici, C. Sherborne, G.C. Reilly, F. Claeyssens, Emulsion templated scaffolds manufactured from photocurable polycaprolactone, Polymer 175 (2019) 243–254.
[13] S. San Manley, et al., New insights into the relationship between internal phase level of emulsion templates and gas–liquid permeability of interconnected macroporous polymers, Soft Matter 5 (2009) 4780–4787.
[14] A. Menner, R. Powell, A. Bismarck, Open porous polymer foams via inverse emulsion polymerization: should the definition of high internal phase (ratio) emulsions Be extended? Macromolecules 39 (2006) 2034–2035.
[15] K.J. Lissant, The geometry of high-internal-phase-ratio emulsions, J. Colloid Interface Sci. 22 (1966) 462–468.
[16] B. Aldemir Dikici, G.C. Reilly, F. Claeyssens, Boosting the osteogenic and angiogenic performance of multiscale porous polycaprolactone scaffolds by in vitro generated extracellular matrix decoration, ACS Appl. Mater. Interfaces 12 (2020) 12510–12524.
[17] W. Busby, N.R. Cameron, C.A.B. Jahoda, Emulsion-Derived foams (PolyHIPEs) containing poly(ε-caprolactone) as matrixes for tissue engineering, Biomacromolecules 2 (2001) 154–164.
[18] S. Changotade, et al., Preliminary in vitro assessment of stem cell compatibility with cross-linked poly(ε-caprolactone urethane) scaffolds designed through high internal phase emulsions, Stem Cell. Int. 2015 (2015), e283796.
[19] E.M. Christenson, W. Soofi, J.L. Holm, N.R. Cameron, A.G. Mikos, Biodegradable fumarate-based PolyHIPEs as tissue engineering scaffolds, Biomacromolecules 8 (2007) 3806–3814.
[20] S. Dikici, et al., Assessment of the angiogenic potential of 2-deoxy-D-ribose using a novel in vitro 3D dynamic model in comparison with established in vitro assays, Front. Bioeng. Biotechnol. 7 (2020).
[21] Y. Hu, et al., Facile preparation of bioactive nanoparticle/poly(ε-caprolactone) hierarchical porous scaffolds via 3D printing of high internal phase Pickering emulsions, J. Colloid Interface Sci. 545 (2019) 104–115.
[22] D.W. Johnson, et al., Macrostructuring of emulsion-templated porous polymers by 3D laser patterning, Adv. Mater. 25 (2013) 3178–3181.
[23] E. Lovelady, S. D. Kimmins, J. Wu, N. R. Cameron, Preparation of emulsion-templated porous polymers using thiol –ene and thiol –yne chemistry, Polym. Chem. 2 (2011) 559–562.
[24] A. Malayeri, et al., Osteosarcoma growth on trabecular bone mimicking structures manufactured via laser direct write, Int. J. Bioprinting 2 (2016).
[25] R. Owen, et al., Emulsion templated scaffolds with tunable mechanical properties for bone tissue engineering, J. Mech. Behav. Biomed. Mater. 54 (2016) 159–172.
[26] N.A. Sears, P.S. Dhavalikar, E.M. Cosgriff-Hernandez, Emulsion inks for 3D printing of high porosity materials, Macromol. Rapid Commun. 37 (2016) 1369–1374.
[27] M. Sušec, S.C. Ligon, J. Stampfl, R. Liska, P. Krajnc, Hierarchically porous materials from layer-by-layer photopolymerization of high internal phase emulsions, Macromol. Rapid Commun. 34 (2013) 938–943.
[28] D. W. Johnson, et al., Fully biodegradable and biocompatible emulsion templated polymer scaffolds by thiol-acrylate polymerization of polycaprolactone macromonomers, Polym. Chem. 6 (2015) 7256–7263.
[29] T. Yang, Y. Hu, C. Wang, B.P. Binks, Fabrication of hierarchical macroporous biocompatible scaffolds by combining pickering high internal phase emulsion templates with three-dimensional printing, ACS Appl. Mater. Interfaces 9 (2017) 22950–22958.
[30] M. Mabrouk, H.H. Beherei, D.B. Das, Recent progress in the fabrication techniques of 3D scaffolds for tissue engineering, Mater. Sci. Eng. C 110 (2020), 110716.
[31] R. Akhtar, M.J. Sherratt, J.K. Cruickshank, B. Derby, Characterizing the elastic properties of tissues, Mater. Today 14 (2011) 96–105.

[32] S. Pashneh-Tala, et al., Synthesis, characterization and 3D micro-structuring via 2-photon polymerization of poly(glycerol sebacate)-methacrylate–an elastomeric degradable polymer, Front. Physiol. 6 (2018).
[33] S. Pashneh-Tala, R. Moorehead, F. Claeyssens, Hybrid manufacturing strategies for tissue engineering scaffolds using methacrylate functionalised poly(glycerol sebacate), J. Biomater. Appl. 34 (2020) 1114–1130.
[34] International Organisation for Standardisation, BS ISO 37:2011 - Rubber, Vulcanized or Thermoplastic. Determination of Tensile Stress-Strain Properties, International Organisation for Standardisation, 2011.
[35] D.H. Ramos-Rodriguez, S. MacNeil, F. Claeyssens, I. Ortega Asencio, Delivery of bioactive compounds to improve skin cell responses on microfabricated electrospun microenvironments, Bioengineering 8 (2021) 105.
[36] M. Frydrych, S. Román, S. MacNeil, B. Chen, Biomimetic poly(glycerol sebacate)/poly(l-lactic acid) blend scaffolds for adipose tissue engineering, Acta Biomater. 18 (2015) 40–49.
[37] Y. Li, W.D. Cook, C. Moorhoff, W.-C. Huang, Q.-Z. Chen, Synthesis, characterization and properties of biocompatible poly(glycerol sebacate) pre-polymer and gel, Polym. Int. 62 (2013) 534–547.
[38] J.L. Ifkovits, et al., Biodegradable fibrous scaffolds with tunable properties formed from photo-cross-linkable poly(glycerol sebacate), ACS Appl. Mater. Interfaces 1 (2009) 1878–1886.
[39] J.L. Ifkovits, R.F. Padera, J.A. Burdick, Biodegradable and radically polymerized elastomers with enhanced processing capabilities, Biomed. Mater. 3 (2008), 034104.
[40] C.L.E. Nijst, et al., Synthesis and characterization of photocurable elastomers from poly(glycerol-co-sebacate), Biomacromolecules 8 (2007) 3067–3073.
[41] Y. Wang, G.A. Ameer, B.J. Sheppard, R. Langer, A tough biodegradable elastomer, Nat. Biotechnol. 20 (2002) 602–606.
[42] H.H. Chen, E. Ruckenstein, Effect of the nature of the hydrophobic oil phase and surfactant in the formation of concentrated emulsions, J. Colloid Interface Sci. 145 (1991) 260–269.
[43] J.-H. Chen, T.T.M. Le, K.-C. Hsu, Application of PolyHIPE membrane with tricaprylmethylammonium chloride for Cr(VI) ion separation: parameters and mechanism of transport relating to the pore structure, Membranes 8 (2018) 11.
[44] D. David, M.S. Silverstein, Porous polyurethanes synthesized within high internal phase emulsions, J. Polym. Sci. Part Polym. Chem. 47 (2009) 5806–5814.
[45] Y. Lumelsky, I. Lalush-Michael, S. Levenberg, M.S. Silverstein, A degradable, porous, emulsion-templated polyacrylate, J. Polym. Sci. Part Polym. Chem. 47 (2009) 7043–7053.
[46] S. Caldwell, et al., Degradable emulsion-templated scaffolds for tissue engineering from thiol–ene photopolymerisation, Soft Matter 8 (2012) 10344–10351.
[47] R.S. Labow, E. Meek, J.P. Santerre, Differential synthesis of cholesterol esterase by monocyte-derived macrophages cultured on poly(ether or ester)-based poly(urethane)s, J. Biomed. Mater. Res. 39 (1998) 469–477.
[48] P.M. Crapo, Y. Wang, Physiologic compliance in engineered small-diameter arterial constructs based on an elastomeric substrate, Biomaterials 31 (2010) 1626–1635.
[49] W. Wu, R.A. Allen, Y. Wang, Fast-degrading elastomer enables rapid remodeling of a cell-free synthetic graft into a neoartery, Nat. Med. 18 (2012) 1148–1153.
[50] S. Dikici, B.A. Dikici, S. MacNeil, F. Claeyssens, Decellularised extracellular matrix decorated PCL PolyHIPE scaffolds for enhanced cellular activity, integration and angiogenesis, Biomater. Sci. 9 (2021) 7297–7310.
[51] B. Aldemir Dikici, et al., Thiolene- and polycaprolactone methacrylate-based polymerized high internal phase emulsion (PolyHIPE) scaffolds for tissue engineering, Biomacromolecules 23 (2022) 720–730.
[52] N. Sengokmen Ozsoz, S. Pashneh-Tala, F. Claeyssens, Optimization of a high internal phase emulsion-based resin for use in commercial vat photopolymerization additive manufacturing, 3D Print. Addit. Manuf. (2023), https://doi.org/10.1089/3dp.2022.0235.
[53] P. Zhao, et al., Research on the electrospun foaming process to fabricate three-dimensional tissue engineering scaffolds, J. Appl. Polym. Sci. 135 (2018), 46898.
[54] M.K. Joshi, et al., Multi-layered macroporous three-dimensional nanofibrous scaffold via a novel gas foaming technique, Chem. Eng. J. 275 (2015) 79–88.
[55] A. Kramschuster, L.-S. Turng, An injection molding process for manufacturing highly porous and interconnected biodegradable polymer matrices for use as tissue engineering scaffolds, J. Biomed. Mater. Res. B Appl. Biomater. 92B (2010) 366–376.
[56] P. Gupta, B.B. Mandal, Tissue-engineered vascular grafts: emerging trends and technologies, Adv. Funct. Mater. 31 (2021), 2100027.
[57] S. Pashneh-Tala, S. MacNeil, F. Claeyssens, The tissue-engineered vascular graft—past, present, and future, Tissue Eng. Part B Rev. 22 (2015) 68–100.
[58] K.-W. Lee, D.B. Stolz, Y. Wang, Substantial expression of mature elastin in arterial constructs, Proc. Natl. Acad. Sci. USA 108 (2011) 2705–2710.
[59] T. Fukunishi, et al., Preclinical study of patient-specific cell-free nanofiber tissue-engineered vascular grafts using 3-dimensional printing in a sheep model, J. Thorac. Cardiovasc. Surg. 153 (2016) 924–932.
[60] E. Yeung, et al., In vivo implantation of 3-dimensional printed customized branched tissue engineered vascular graft in a porcine model, J. Thorac. Cardiovasc. Surg. 159 (2020) 1971–1981.e1.
[61] K. Christensen, et al., Freeform inkjet printing of cellular structures with bifurcations, Biotechnol. Bioeng. 112 (2015) 1047–1055.
[62] B. Duan, L.A. Hockaday, K.H. Kang, J.T. Butcher, 3D Bioprinting of heterogeneous aortic valve conduits with alginate/gelatin hydrogels, J. Biomed. Mater. Res. 101A (2013) 1255–1264.
[63] T.J. Hinton, et al., Three-dimensional printing of complex biological structures by freeform reversible embedding of suspended hydrogels, Sci. Adv. 1 (2015), e1500758.
[64] S. Krishnamoorthy, S. Wadnap, B. Noorani, H. Xu, C. Xu, Investigation of gelatin methacrylate working curves in dynamic optical projection stereolithography of vascular-like constructs, Eur. Polym. J. 124 (2020), 109487.
[65] S. Krishnamoorthy, Z. Zhang, C. Xu, Biofabrication of three-dimensional cellular structures based on gelatin methacrylate–alginate interpenetrating network hydrogel, J. Biomater. Appl. 33 (2019) 1105–1117.
[66] C. Norotte, F.S. Marga, L.E. Niklason, G. Forgacs, Scaffold-free vascular tissue engineering using bioprinting, Biomaterials 30 (2009) 5910–5917.
[67] A.G. Tabriz, M.A. Hermida, N.R. Leslie, W. Shu, Three-dimensional bioprinting of complex cell laden alginate hydrogel structures, Biofabrication 7 (2015), 045012.
[68] R. Xiong, Z. Zhang, W. Chai, Y. Huang, D.B. Chrisey, Freeform drop-on-demand laser printing of 3D alginate and cellular constructs, Biofabrication 7 (2015), 045011.
[69] R. Wang, et al., Freestanding hierarchical vascular structures engineered from ice, Biomaterials 192 (2019) 334–345.
[70] J. Visser, et al., Biofabrication of multi-material anatomically shaped tissue constructs, Biofabrication 5 (2013), 035007.
[71] Y.-L. Wu, et al., Three-dimensional printing of poly(glycerol sebacate) acrylate scaffolds via digital light processing, ACS Appl. Bio Mater. 3 (2020) 7575–7588.